

RSC Advances



This is an *Accepted Manuscript*, which has been through the Royal Society of Chemistry peer review process and has been accepted for publication.

Accepted Manuscripts are published online shortly after acceptance, before technical editing, formatting and proof reading. Using this free service, authors can make their results available to the community, in citable form, before we publish the edited article. This *Accepted Manuscript* will be replaced by the edited, formatted and paginated article as soon as this is available.

You can find more information about *Accepted Manuscripts* in the [Information for Authors](#).

Please note that technical editing may introduce minor changes to the text and/or graphics, which may alter content. The journal's standard [Terms & Conditions](#) and the [Ethical guidelines](#) still apply. In no event shall the Royal Society of Chemistry be held responsible for any errors or omissions in this *Accepted Manuscript* or any consequences arising from the use of any information it contains.



Polymer Chemistry

ARTICLE

PVAc/PEDOT:PSS/Graphene-Iron Oxide Nanocomposite (GINC): An Efficient Thermoelectric Material

Received 00th
January 20xx,

Abhijit Dey,^{a,*} Arunava Maity,^b Md Abdul Shafeeuulla Khan,^a Arun Kanti Sikder,^a Santanu Chattopadhyay^{c,*}

Accepted 00th January 20xx

DOI: 10.1039/x0xx00000x

www.rsc.org/

A green method for graphene-iron oxide nanocomposite (GINC) synthesis and its PVAc based polymer nanocomposites is reported in earlier communication. The fabricated PVAc-GINC film exhibited a conductivity of 2.18×10^4 S/m with a Seebeck coefficient of 38.8 μ V/K. Hence, the power factor (PF) reached to a tune of 32.90μ W $m^{-1}K^{-2}$ which is 27 fold higher than the thermoelectric material based on PVAc-graphene composite as reported in the contemporary literature. In continuation to above mentioned study PEDOT:PSS was used to further enhancement of power factor (PF) and figure of merit (ZT) of the system. During evaluation, PEDOT:PSS/GINC composite (5:95) showed remarkable increase in various thermoelectric properties like electrical conductivity 8.0×10^4 S/m with a Seebeck coefficient of 25.42 μ V/K and thermal conductivity 0.90 W/mK. Hence PF and ZT reach upto 51.93 μ W/mK² and 0.017 respectively. To improve the mechanical strength of the polymer composite, cellulose fibre has also been employed. By addition of cellulose fibre, though mechanical strength of the composite increases but PF reached to 5.6, which is 10 times lower than the PEDOT:PSS/GINC composite

Utilizing a thermoelectric (TE) material, a potential difference is developed exploiting a temperature difference or temperature difference can be improvised by the application of voltage¹. The TE performance of a material is expressed by the dimensionless figure of merit, i.e. ZT, which is defined as $S^2\sigma/\kappa$ where 'S' denoted by thermopower i.e. Seebeck coefficient, σ is denoted by electrical conductivity, κ is thermal conductivity and T is absolute temperature⁸. Because of low κ value of conductive polymers compared to commonly utilized TE inorganic materials, such as Bi₂Te₃-based materials, conductive polymers became prospective candidates for tailoring properties TE materials. Additionally, conductive polymers possess some other beneficial features like low density, low cost, less toxicity, relatively straightforward synthesis and easy processing into versatile forms².

Several researchers across the globe have been trying to jeer out effective properties out of graphene since its invention in 2004¹. Unique properties of graphene attracted widespread attention for its high carrier mobility², room temperature quantum effect and ambipolar electric field effect. If the layers present in the graphite restricted to fewer i.e. 10 or less, the resultant entity is known as graphene. Such graphene shows exceptional properties which is reduced drastically by increasing the number of graphene layers until reaches to 3D form³⁻⁴ i.e. graphite. Due to such distinct properties, graphene has become one of the interesting material

for electronic composite and advance mechanical resonator^{6,7}. Additionally, graphene shows excellent electrical, optical, and thermal properties¹. A high Seebeck coefficient has been predicted in a graphene-based nanostructure⁹ and the electrical conductance of graphene is comparable to that of copper.¹⁰ A large scale production of graphene sheets has been reported in the literature.¹¹ These factors makes graphene as a frontrunner for futuristic thermoelectric applications. However, the ability of graphene to conduct heat is an order of magnitude larger than that of copper.¹² Therefore, it is mandatory to restrain its thermal conductance for its TE application. The high thermal conductance of graphene is mainly due to the contribution of lattice, whereas the electronic contribution to the thermal conduction can be ignored.¹² Therefore, suitable engineering of phonon transport properties makes it possible to diminish the total thermal conductance without considerable reduction of the electrical conductance and the power factor. Computational studies performed on the thermal conductivity of graphene-based structures has revealed that boundaries and edge irregularity can strongly persuade the thermal conductance^{14,15}. Further, the considerable effects on thermal conductance have been observed due to defects, vacancy, isotope doping, and hydrogen passivation.¹⁵⁻¹⁷

Higher power factor can be assimilated by two mechanisms in polymer based composites. Polymer doping¹⁸⁻²⁰ and blending with different conducting nano fillers²¹⁻²³ like CNT²⁴⁻²⁵ and graphenes²⁶⁻²⁹. TE properties of these polymer composites can be upgraded to be comparable to that of chalcogenides. However, their competence is still inferior for many reasons.^{18, 21, 22} High intrinsic electrical conductivity makes poly(3-hexylthiophene)(P3HT)³¹, polyaniline (PANI)^{18, 32-34}, and (3,4-ethylenedioxythiophene): poly(styrenesulfonate) (PEDOT:PSS)³⁰, useful. The electrical properties of the polymer can simply be

^a High Energy Materials Research Lab, EMR Division, Sutarwadi, Pune, India

^b Organic Chemistry Division, CSIR-NCL, Pune, Maharashtra

^c Rubber Technology Centre, IIT Kharagpur, West Bengal, India

† Footnotes relating to the title and/or authors should appear here.

Electronic Supplementary Information (ESI) available: [details data table for various composition, reported values of other organic/inorganic composite and their references]. See DOI: 10.1039/x0xx00000x

enhanced without disturbing the thermal conductivity and mechanical flexibility.³⁵ Percolation theory predicts a drastic increase in electrical conductivity after reaching to a percolation threshold.³⁶⁻³⁷

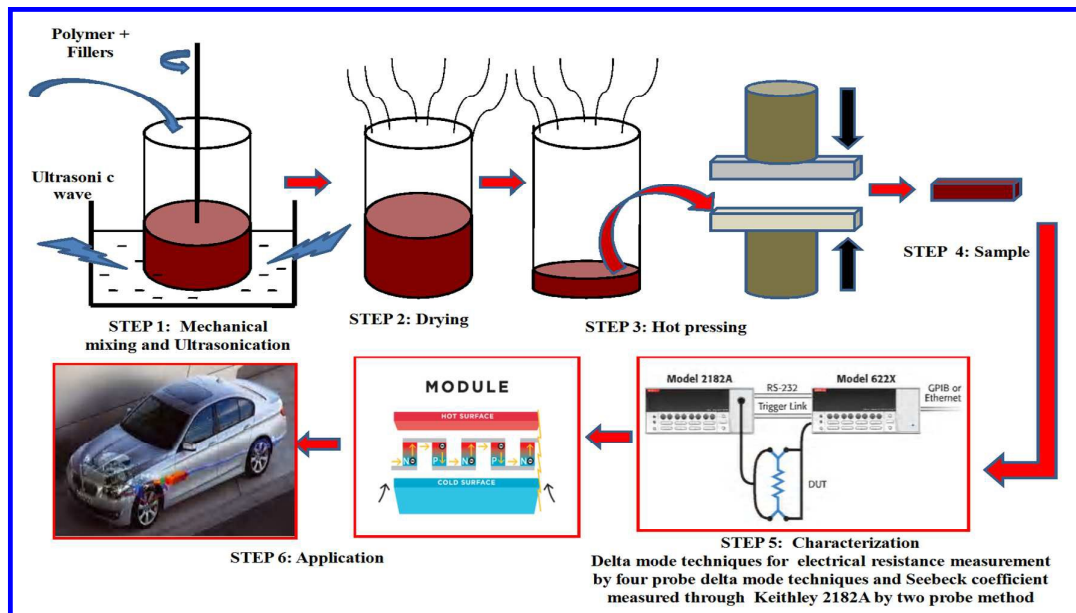
Simple preparation method of GINC involves the solvo-thermal reaction³⁸. We have recently prepared GINC with a novel method. The novelty is due to its simplicity, economic nature and eco-friendliness. A comprehensive study of thermoelectric properties (electrical conductivity, Seebeck coefficient, thermal conductivity, power factor and Figure of merit) of PVAc, PEDOT: PSS and PVAc/PEDOT: PSS polymer with different fillers like GINC, graphene have been evaluated and presented. Additionally, cellulose based polymer composite have been formulated and evaluated for thermoelectric properties.

In spite of high thermal conductivity, such materials could be engineered in a simple way to enhance thermoelectric properties of synthesized polymer nanocomposite. PVAc was chosen because of its good adhesive nature and binding capability with lower thermal conductivity. Such properties help to increase the filler loading and efficiency of thermoelectric material. To increase the electrical conductivity efficiently, graphene has been used as a substrate. It is known that metal oxides such as iron oxide nickel oxide, cadmium oxide and doped zirconium oxide has shown impressive TE properties for various application.⁴⁰ Amongst these oxides, thermoelectric properties Fe_2O_3 has been studied well in the literature. It has been observed that Fe_2O_3 can be a promising transition metal oxide for TE application as it exhibits high

thermoelectric power factor at room as well as elevated temperatures. Fe_2O_3 thin films have shown peak Seebeck coefficient of $1650 \mu\text{V}/\text{K}$ in the temperature range of 270-290 K. A peak electrical conductivity of $5.5 \times 10^3 \text{ S}/\text{m}$ has been reported in the same temperature range, resulting to a large PF of $1.5 \times 10^4 \mu\text{W}/\text{m}\cdot\text{K}^2$. Nano Fe_2O_3 was decorated over the graphene sheet during exfoliation of GINC. After decoration, the staking nature of graphene sheet was supposed to reduce drastically which ultimately reduce the thermal conductivity as well as tendency of graphene to graphite transformation. PEDOT:PSS has been incorporated as conducting polymer in different concentrations and optimization has also been carried out to upsurge the TE efficiency. Conducting polymer helps to modulate the junction which makes intact the electrical network but obstructs thermal network. Further cellulose fibres were tried to be used to increase its mechanical properties of the nanocomposite.

Experimental: Synthesis of PVAc/PEDOT: PSS- GINC Composite

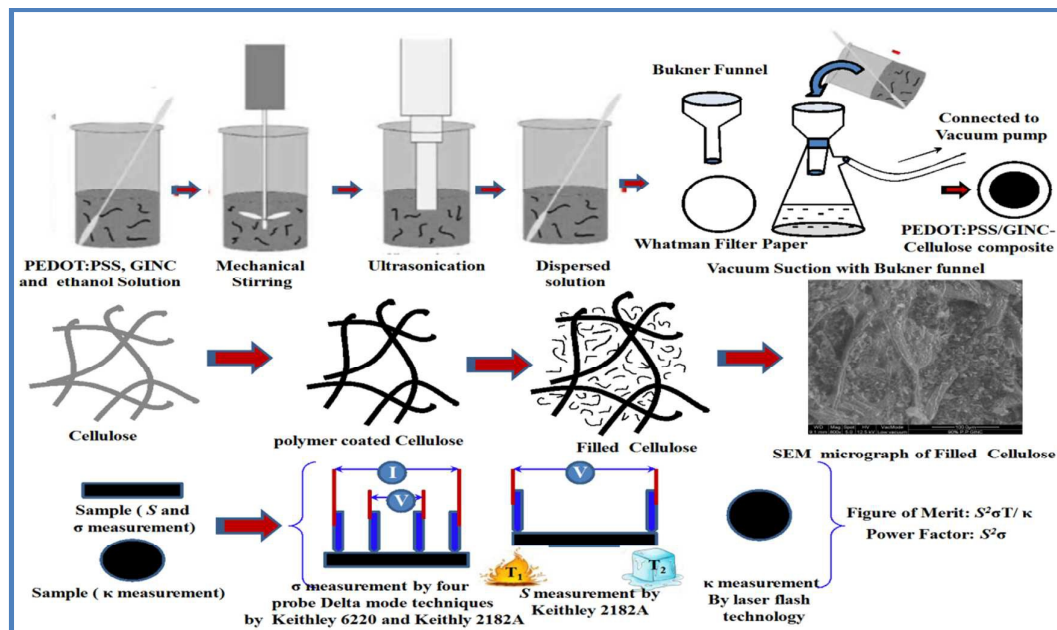
Nano iron oxide and nano graphene were prepared separately during preparation of GINC nanocomposite(Graphene:Iron oxide::1:1). The detail synthesis procedure can be find in our earlier article.^{39, 48} In the present study, we have made polymer composite based on PEDOT: PSS(conductive grade, 1.3 wt.% in H_2O , σ :1 S/cm make: Sigma Aldrich)/PVAc/PEDOT:PSS and GINC. The detail synthetic methodology, characterization and applications have been emphasized in Scheme 1.



Scheme 1: Synthesis procedure of PVAc/PEDOT:PSS- GINC Composite, its evaluation and possible application

To improve the mechanical strength, cellulose fibre has been employed. The detail synthetic procedure and characterization have been highlighted in scheme 2. The optimised composition based on 5% PEDOT:PSS and 95% GINC, have been used in ethanol solution. To achieve better dispersion, mechanical stirring and ultrasonication have been carried out. Then, dispersed solution was

passed through the watmann filter paper with the help of Buchner funnel. During suction, filler particles adsorbed on the filter paper making a conducting network for electrical conduction. After drying, the formed composite samples have been prepared with required dimension and evaluated their thermoelectric properties.

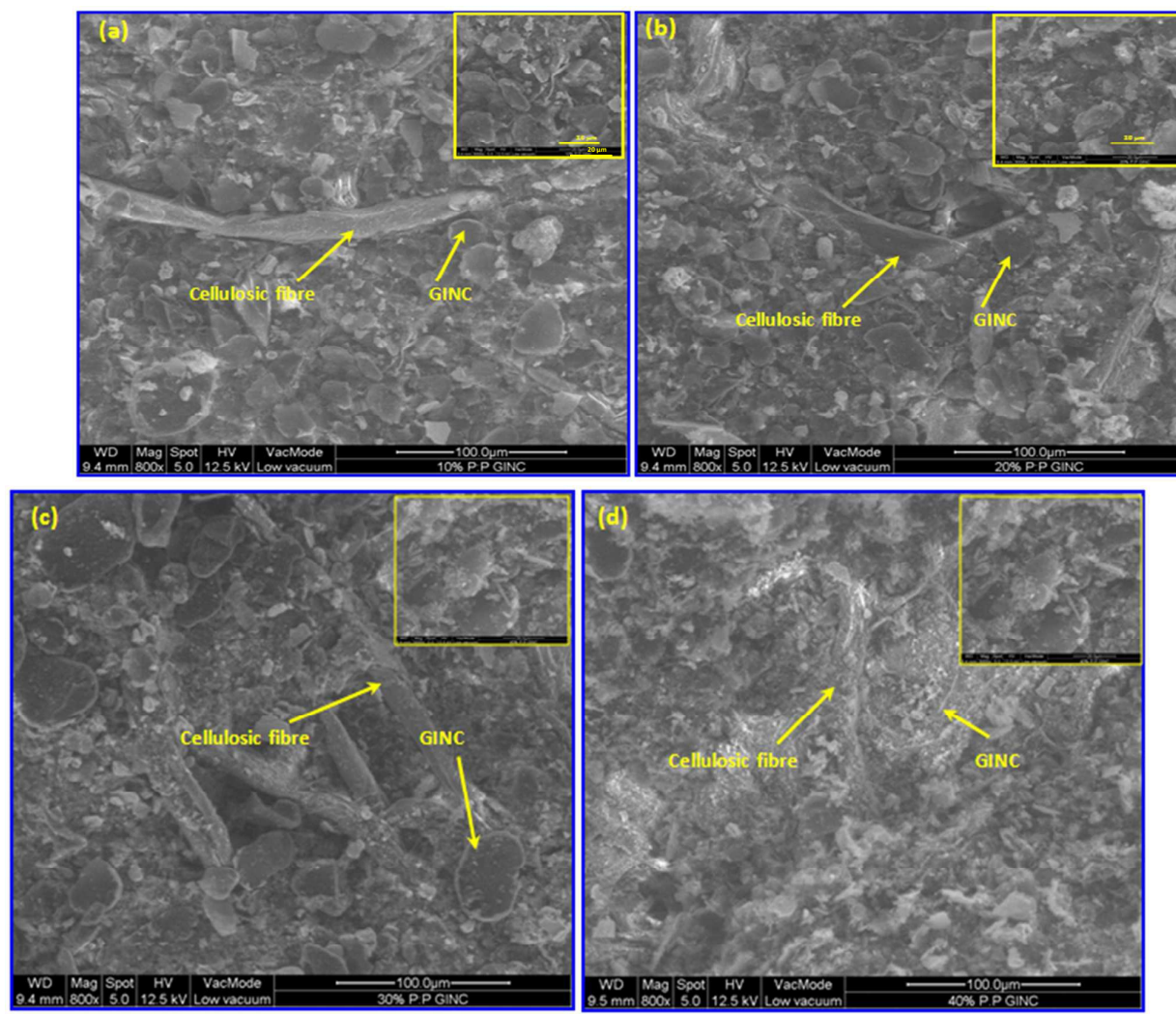


Scheme 2: Synthesis procedure of cellulose based PVAc/PEDOT:PSS- GINC Composite

Characterization of polymer GINC composite

Environmental scanning electron microscopy (ESEM) images with different magnification (800X and inset, 3000X) have been presented in Figure 1. Figure 1 consists of different micrographs of various cellulose polymer GINC nanocomposites with concentration variation of polymer GINC nanocomposites. Micrograph shows that cellulosic fibre and pore were filled with polymer-GINC composite. It shows continuous dispersion of PEDOT:PSS/GINC over the cellulosic film.

Inset of the micrographs highlighted continuous network formation between cellulosic fibre and polymer GINC composite. As concentration increases, coating ability of polymer GINC over cellulosic fibre enhances drastically. Hence effective conductive network has been formed. Hence efficiency gets enhanced. Figure 1j represents the simple cellulosic film. Small pores are visible in this micrograph.



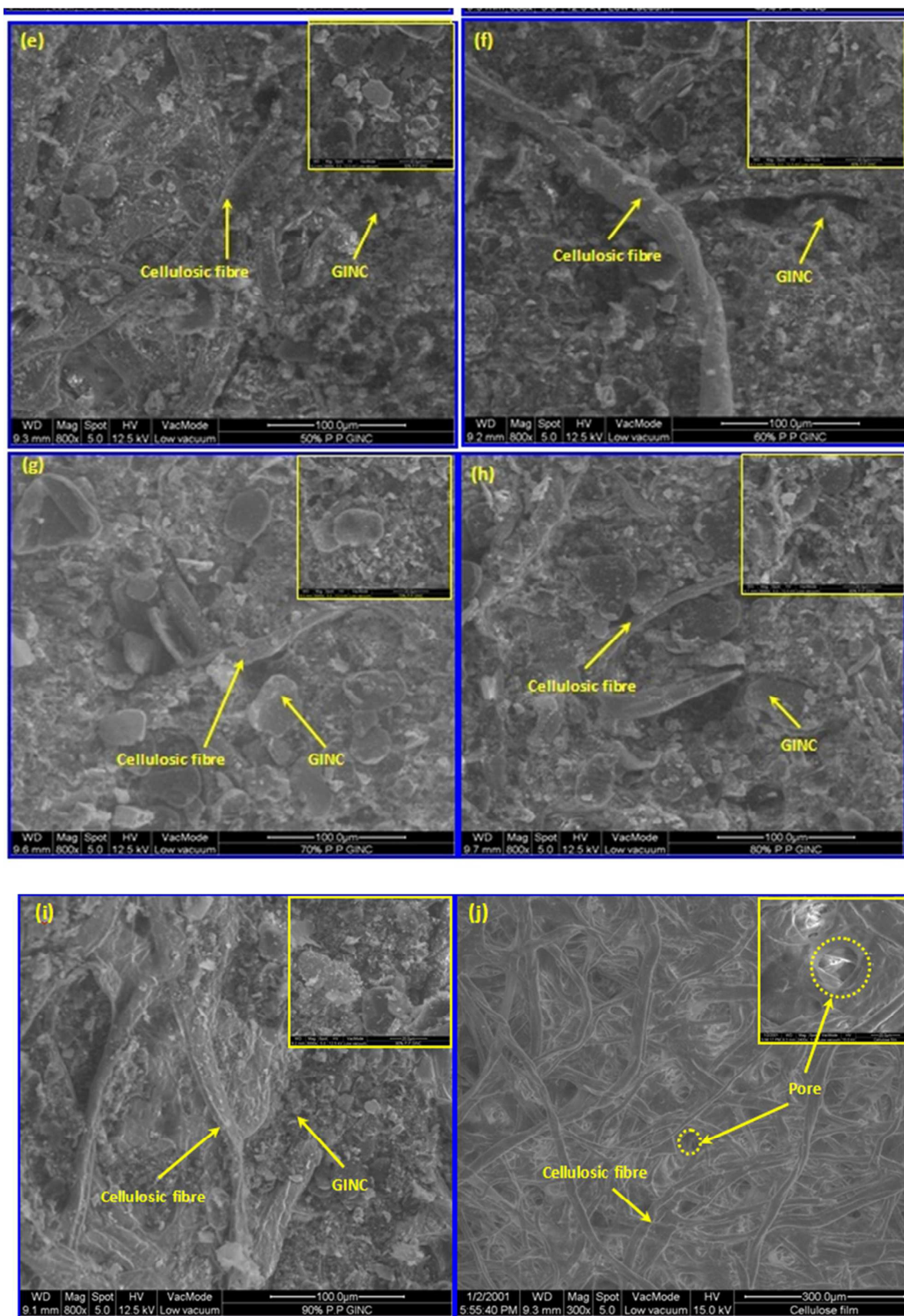


Figure 1: Environmental scanning electron micrographs at 800X and 3000X magnification (inset) of cellulose polymer GINC based composite with (a) 10% PEDOT:PSS solution (b) 20% PEDOT:PSS solution (c) 30% PEDOT:PSS solution (d) 40% PEDOT:PSS solution (e) 50% PEDOT:PSS solution (f) 60% PEDOT:PSS solution (g) 70% PEDOT:PSS solution (h) 80% PEDOT:PSS solution (i) 90% PEDOT:PSS solution and (j) cellulosic film

Band gap measurement: To examine optical energy gap of the synthesized compounds, optical diffuse reflectance measurements were performed on finely grounded powders at room temperature. The spectra were recorded at the range of 200 nm to 800 nm using a Cary 5000 UV-Vis spectrometer. Absorption (α/Λ) data were calculated from reflectance data using Kubelka-Munk equations:

$\alpha/\Lambda = (1 - R)^2/(2R)$, where R is the reflectance and α and Λ are the absorption and scattering coefficients, respectively. Finally the energy band gaps were derived from α/Λ vs. E (eV) plots. The detailed graphical representation is depicted in Figure 2. The detailed assignments of those are highlighted in Table 1.

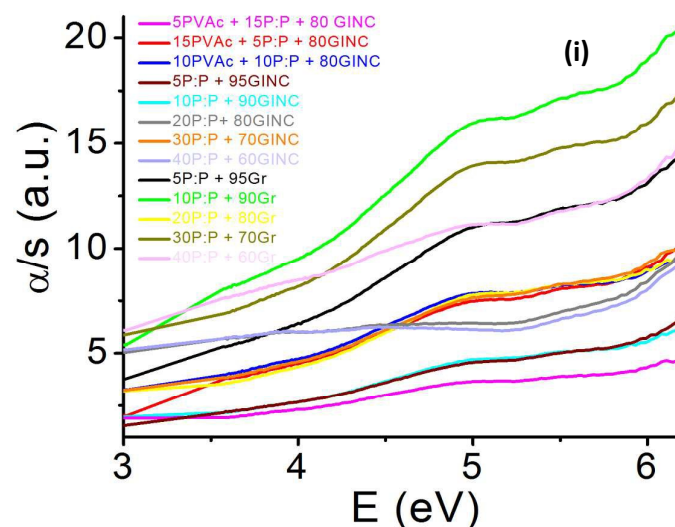


Table 1 Optical band gaps for various compositions.

Sr No	Sample Name	Band Gap (eV)
1	10P:P + 90Gr	3.04
2	30P:P + 70Gr	3.06
3	5P:P + 95Gr	3.12
4	10PVAc + 10P:P + 80GINC	3.13
5	20P:P + 80Gr	3.20
6	15PVAc + 5P:P + 80GINC	3.11
7	30P:P + 70GINC	3.07
8	20P:P + 80GINC	3.25
9	40P:P + 60GINC	3.31
10	10P:P + 90GINC	3.27
11	5P:P + 95GINC	3.26
12	5PVAc + 15P:P + 80 GINC	3.32
13	40P:P + 60Gr	3.02

P:P= PEDOT:PSS, Gr= Graphene, GINC= Graphene iron oxide nanopposite

Figure2: (i) Graphical representation of energy band gap derived from α/Λ vs. E (eV) plots. Table 1: tabulated representation of band gap for various composition

In general, electrical conductivity and seebeck coefficient increases with decreases of band gap. In the above table, mild variations were observed in band gap calculation. Hence, it is very difficult to correlate any relationship between band gap and electrical conductivity

Thermoelectric Application of polymer based GINC and Cellulosic polymer based GINC

Thermoelectric properties are of parameters, viz. Seebeck coefficient or thermopower, electrical conductivity, thermal conductivity helps to measure the PF and ZT.

Thermoelectric Power/ Seebeck coefficient (S) Measurements.

To calculate the thermopower as a function of temperature, samples of the polymer nanocomposite film as well as cellulosic polymer nanocomposite with dimensions of 30mm \times 6 mm \times 1 mm were cut and placed on a thermally insulating fibre glass. A Peltier heater was placed at one end of the sample with a thermally conductive epoxy (electrically insulating 2763 Stycast), while the other end, a piece of copper (drainage of heat) to make a contact with the Peltier cooling module. The temperature gradient and voltage drop along the film was measured with thermocouples arranged in series (electrically insulated from the sample with 2763 Stycast) with two copper wires. To make sure that the thermal gradient and the voltage drop were being measured at the same place, two small Cu films were attached to the polymer-GINC film

with thermally/electrically conducting silver epoxy (Dupont 4929N). The thermocouple and the voltage wires were attached to these Cu films. The thermoelectric voltages were scrutinized with respect to temperature difference by Keithley 2182A nanovoltmeter. The base temperature was altered with Peltier cooling module. Two independent methods have been adopted to determine the thermoelectric power: 1. after reaching a stable state through an applied current to the heater and 2. by fitting the linear V vs ΔT response to a heating pulse. The unconventionality between both methods and different experimentation was always lower than 5%. A highly sensitive IR camera was used to measure the temperature gradient along the sample.

Electrical Resistivity Measurements: Due to the high electrical conductive nature of the composite, delta mode four probe methods have been used to measure the electrical resistivity. The smallest possible current (100mA) was obtained by Keithley 6220 and voltage was monitored with a Keithley 2182A nanovoltmeter. To avoid heating of the sample at low temperature, the smallest possible current was used. Polymer nanocomposite sample with a

dimension of 8mm × 3mm × 1mm have been prepared and subjected to the test to measure electrical conductivity. The sample were tested several times within one month interval. The properties were found to be consistent. These reflects the sample stability under room temperature and atmosphere

Remarkable increase in electrical conductivity (6.7×10^4 S/m) of PEDOT:PSS/GINC composite have been achieved (Figure 3d). Thermal conductivity and Seebeck coefficient have been affected by small degree. Raw PVAc is having an electrical conductivity of 10^{-13} S/m and the electrical conductivity was calculated at ambient

conditions. Results have been reproduced even after two months indicating good stability of the nanocomposite with a period of time. The Seebeck coefficient (see Fig. 3b) also exhibits interesting trend with initial decrease and then the final increase to reach to a maximum with 20 wt. % PEDOT:PSS concentration. Fig. 3c exhibits, the variation of power factor (PF) as a function of filler concentration. According to Fig. 3c, PF increases and reaches to a very high value, $34.17 \mu\text{W m}^{-1}\text{K}^{-2}$ at 20 wt.% filler concentration. In the same way, thermoelectric figure of merit i.e. ZT, was found to be maximum i.e. 0.003.

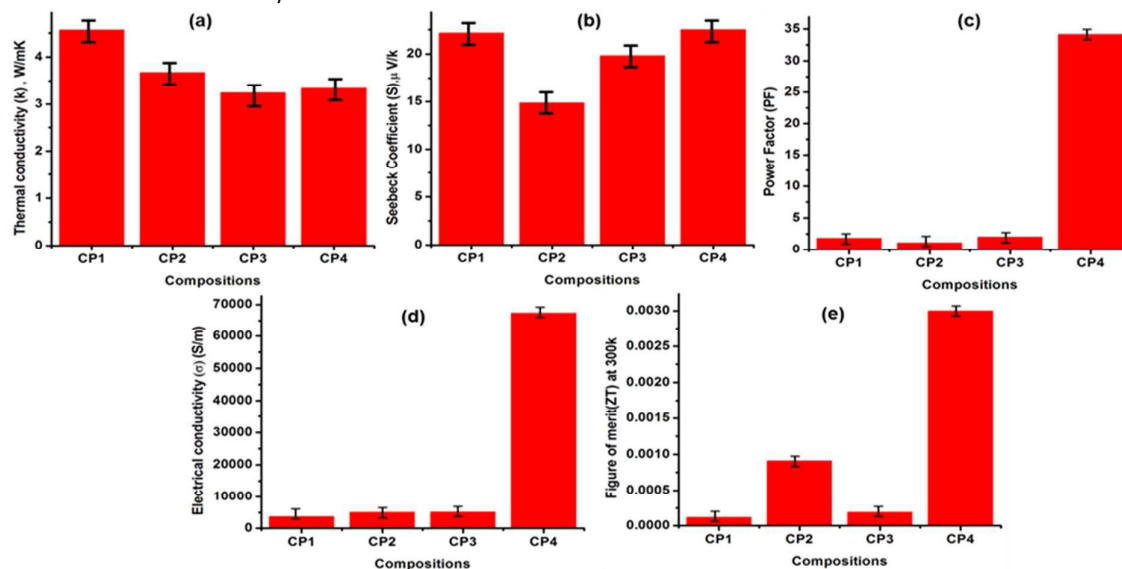


Fig. 3: (a) Thermal conductivity (b) Seebeck coefficient (c) power factor (d) Electrical conductivity and (e) ZT as a function of PVAc:PEDOT:PSS concentration at room temperature (300K). **CP1:** 15% PVAc+ 5% PEDOT:PSS solution +80% GINC, **CP2:** 10% PVAc+ 10% PEDOT:PSS solution +80% GINC, **CP3:** 5% PVAc+ 15% PEDOT:PSS solution +80% GINC, **CP4:** 20% PEDOT:PSS solution +80% GINC

In Figure 4, five different compositions (CP1 - CP5) containing different concentration of PEDOT:PSS and filler i.e. GINC/graphene (detail compositions and data table is given in ESI, Table S2 and S3) have been evaluated by means of thermal conductivity, electrical conductivity, Seebeck coefficient, power factor and ZT. In graphics of Figure 4a, thermal conductivity of PEDOT:PSS-graphene composite are much higher compare to the PEDOT:PSS-GINC composite which is main drawback for graphene based composite. In other way, seebeck coefficient is also higher for PEDOT:PSS-GINC composite compare to PEDOT:PSS-graphene composite. In the same way, electrical conductivity of PEDOT:PSS-GINC composite have been found to be much higher than PEDOT:PSS-graphene composite. Hence, higher value of PF and ZT have been achieved in concentration level of filler. These phenomena come into play, when two dissimilar materials with a large difference in electrical conductivity are mixed.

case of PEDOT:PSS-GINC composite. Basically, presence of iron oxide nano particle, the thermal conducting network has been destructed but electrical conduction remained unchanged. The reason is that during composite formation electron transport remains intact but phonon transport gets disturbed. During optimization of PEDOT:PSS and GINC concentration in the composite, composition with 5 wt.% PEDOT:PSS solution and 95 wt.% shows very high PF. and ZT value i.e. $51.93 \mu\text{W m}^{-1}\text{K}^{-2}$ and 0.017 respectively. This value is found to be highest ever reported in the literature for PEDOT:PSS based system. The improvement of electrical conductivity was following the percolation law of the composite which predicts an enhancement of electrical conductivity up to a critical

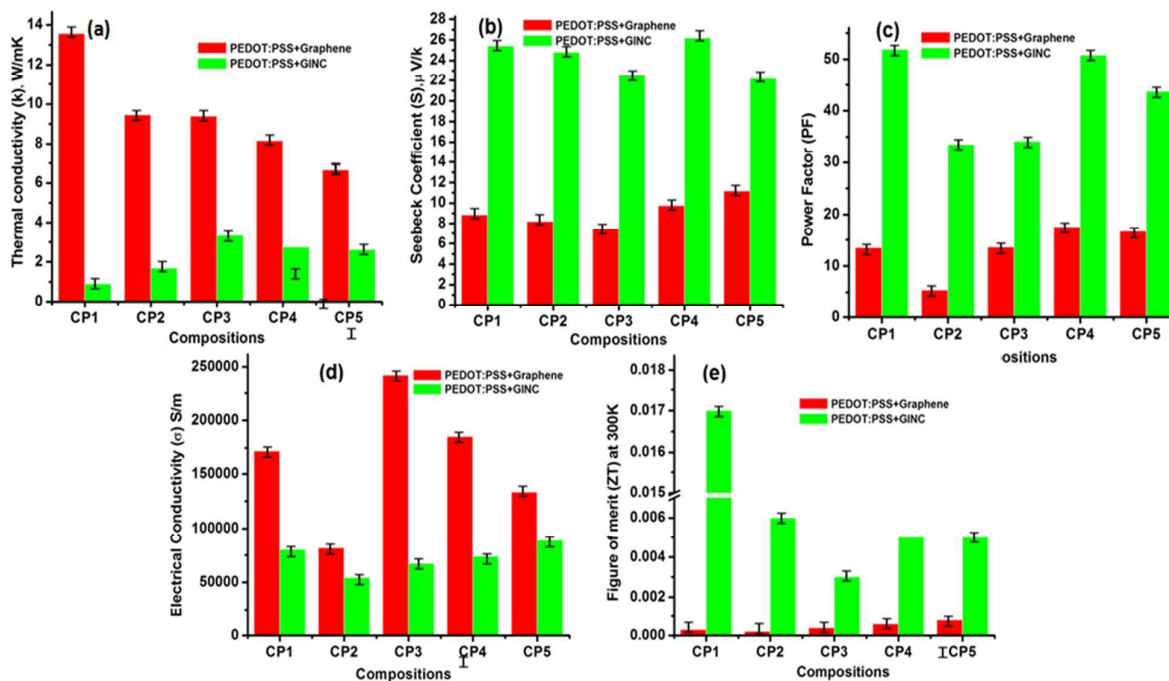


Fig. 4:(a)Thermal conductivity (b)Seebeck coefficient (c) power factor (d)Electrical conductivity and (e) ZT as a function of PEDOT:PSS concentration at room temperature (300K).CP1:5% PEDOT:PSS solution +95% Graphene/GINC,CP2: 10% PEDOT:PSS solution +90% Graphene/GINC CP3:20% PEDOT:PSS solution +80% Graphene/GINC CP4:30% PEDOT:PSS solution +70% Graphene/GINC, CP5:40% PEDOT:PSS solution +60% Graphene/GINC

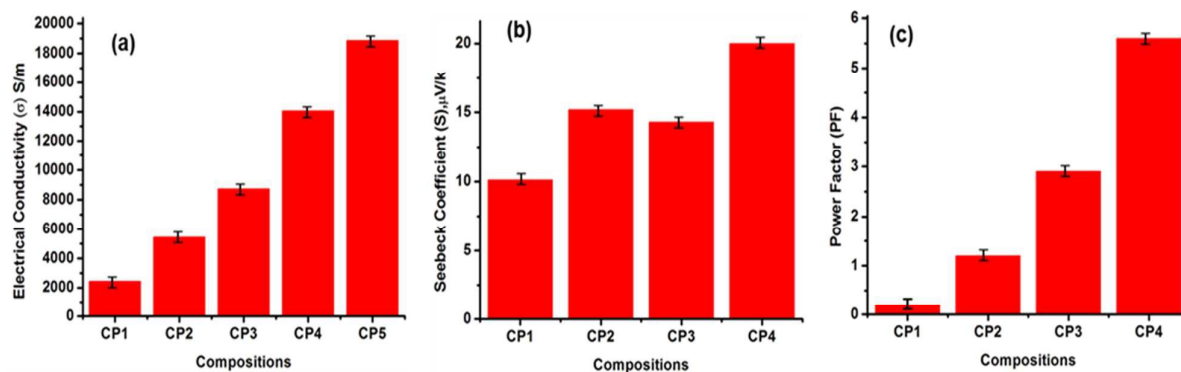


Fig. 5: (a) Electrical conductivity (b) Seebeck coefficient (c) power factor as a function of PEDOT:PSS (5 wt. %) /GINC (95 wt. %) composite. Concentration at room temperature (300K).CP1: Cellulose paper+PEDOT:PSS-GINCcomposite (10 wt. %), CP2: Cellulose paper+ PEDOT:PSS- GINC composite (15 wt. %), CP3: Cellulose paper+ PEDOT:PSS- GINC composite (20 wt. %), CP4: Cellulose paper+ PEDOT:PSS- GINCcomposite (30 wt. %), CP5: Cellulose paper+ PEDOT:PSS- GINC composite (40 wt. %)

Polymer Chemistry

ARTICLE

Figure 5 represents the graphical representation of electrical conductivity, seebeck coefficient and power factor with concentration variation of PEDOT:PSS (5 wt. %) /GINC (95 wt.%) composite in cellulose matrix. Though mechanical strength increases, power factor value is found to be very less compare to the bare composite. During the study of thermoelectric properties, PEDOT:PSS /GINC composite showed atleast 50 fold increases in ZT and four times increase in power factor were observed compared to the PEDOT:PSS-graphene composite with equal filler loading (95wt%). The detail data have been given in S4, ESI. This has been one of the novel findings from this study. In GINC, nano iron oxides were decorated over 2D graphene sheet. Presence of nano iron oxide particle helps to destroy phonon transport network but electron transport network remain intact. When GINC is employed as conducting filler, it only decouples σ and S , but also enhances both the parameter simultaneously. Further, PEDOT: PSS helps to modulate the junction by forming thin layer of coatings. These junction helps to transport electron only, However, the enhancement of Seebeck coefficient is marginal with respect to electrical conductivity in case of PEDOT:PSS/GINC composite. The electrical conductive nature of the PEDOT:PSS assists to enhance

the electrical conductivity and reduces the thermal conductivity of the matrix. During the study, we have understand a unusual mechanism of PEDOT:PSS in presence of GINC. PEDOT:PSS is a polar conducting polymer. PEDOT:PSS is highly compatible with GINC. During preparation of polymer nanocomposite, PEDOT:PSS easily coated over GINC. Hence the interlayer junctions were modulated in such a way that reduces thermal conductivity but increases electrical conductivity and seebeck coefficient, hence increases the power factor. In addition, phonon are responsible for thermal conductivity. Phonone gets scattered during conduction. Hence reduces the thermal conductivity. In PVAc, though its thermal conductivity is comparatively low but efficiency to decreases the thermal conductivity is relatively poor. The reason is, PVAc is a non conducting polymer and it is not sufficiently compatible with GINC. Hence the modulation of interlayer junctions are become difficult. Besides thisd, Phonone scattering is also not effective for PVAc compare to PEDOT:PSS.

A comparative summary of the latest results based on polymer matrix (see Table 1) and other composites of inorganic and organic materials have been highlighted in Table S5 in ESI. Corresponding references have given in S6 in ESI.

Table 1: Summary of thermoelectric properties of various PVAc based carbon material composites.

Sample ⁴⁹	σ , S/m	S , $\mu\text{V}/\text{k}$	κ , W/mK	Calculated PF ($S^2\sigma$) $\mu\text{W m}^{-1}\text{K}^{-2}$
PVAc +CNT (20%) [Ref. 42]	4800 (300K)	40-50 (300K)	0.18-0.34 at 300K	PF= 7.8-12
PVAc+SWCNT (40%) [Ref. 43]	900	40	0.25	PF= 1.44
PVAc+SWCNT (3 wt. %) + GA [Ref: 44]	22-49	39-42	0.22-0.25	PF=0.033
PVAc+Au+ CNT [Ref. 45]	10^5	---	Unaffected	Unaffected
PVAc+ DOC + MWCNT (7-12%)	32-63	5-10	0.13-0.17	PF= 0.34-0.50
PVAc+ TCPP+ MWCNT (7-12%)	10-100	22-26	0.14	PF= 0.079-0.34
PVAc+ DOC + DWCNT (7-12%)	--	50-70	0.15	PF=0.045- 0.096
PVAc+ TCPP + DWCNT (7-12%) [Ref. 46]	--	70-82	0.155-0.16	PF= 0-0.204
PVAc+ polyethyleneimine (10 wt. %) +CNT with 99% purity (20 wt. %) + SDBS (20-60 wt. %),	420-1250	-66- -75	--	PF= 1.89- 7.03
PVAc+ CNT with 99% purity (20 wt.%) + SDBS(20 wt. %) + PEI (0-40 wt. %),	320-430	-65- -80	--	PF= 1.35- 2.752
PVAc+ CNT with 99% purity (20 wt. %) + SDBS (40 wt. %)+ PEI (0-40 wt%), Composition IX [Ref. 47]	440-920	-110 - 110	--	PF= 5.32- 11.13

ARTICLE

Journal Name

PVAc+ Au deposited CNT (0-20 wt. %) +PEDOT: PSS (15% vol. Replacement by Au) [Ref. 45]	6×10^5	2.5	--	PF= 3.75
PEDOT:PSS+ PVAc + CNT(35-75%) [Ref. 41]	5×10^4 $- 1.35 \times 10^5$	19-34	0.2-0.4	PF=30-110
PVAc + GINC (80 wt. %)				
PVAc + Graphene (95%) [Ref: 39]	2.18×10^4 2.89×10^3	38.8 20.7	- -	PF= 32.90 PF= 1.24

Conclusion

In this work, conducting polymer like PEDOT:PSS was used and optimized its concentration to further improvement of properties of polymer-GINC composite by means tailoring of Seebeck coefficient, electrical conductivity, and thermal conductivity. During evaluation, PEDOT:PSS/GINC composite (5:95) shows remarkable increase in various thermoelectric properties like electrical conductivity 8.0×10^4 S/m with a Seebeck coefficient of 25.42 μ V/K and thermal conductivity 0.90 W/mK. Hence PF and ZT reaches upto 51.93 μ W/mK² and 0.017 respectively. Thermal conductivity was measured through the Laser Flash technique is

based on the measure of the thermal transient of the rear surface of the sample when a pulsed laser illuminates the front: in this way it is possible to avoid interferences between the thermal sensor and the heat source. The physical model of the Laser Flash measurement supposes to have a single pulsed heat source (delta like), for example a laser shot, on the sample front surface. The study of the thermal transient of the rear surface provides the desired thermal information. To improve the mechanical strength of the polymer composite, cellulose fibre has been employed. By addition of cellulose fibre, though mechanical strength of the composite increases but PF reaches to 5.6, which is 10 times lower than the PEDOT:PSS/ GINC composite

References

1. K. S. Novoselov, A. K. Geim, S. V. Morozov, D. Jiang, Y. S. Zhang, V. Dubonos, I. V. Grigorieva and A. A. Firsov, *Science*, 2004, **306**, 666.
2. K. S. Novoselov and A. K. Geim, *Nat. Mater.* 2007, **6**, 183.
3. W. Zhang, W. He and X. Jing, *J. Phys. Chem. B*, 2010, **114**, 10368
4. K. S. Novoselov, D. Jiang, F. Schedin, T. J. Booth, V. V. Khotkevich, S. V. Morozov and A. K. Geim, *Proc. Natl. Acad. Sci.* 2005, **102**, 10451.
5. B. Partoens and F. M. Peeters, *Phys. Rev. B: Condens. Matter Mater. Phys.*, 2006, **74**, 075404
6. A. Schlierf, P. Samorì and V. Palermo, *J. Mater. Chem. C* 2014, **2**, 3129.
7. A. K. Geim, *Science* 2009, **324**, 1530.
8. L. D. Zhao, S. H. Lo, Y. Zhang, H. Sun, G. Tan, C. Uher, C. Wolverton, P. V. Dravid and M. G. Kanatzidis, *Nature* 2014, **508**, 373.
9. D. Dragoman and M. Dragoman, *Appl. Phys. Lett.*, 2007, **91**, 203116.
10. J. H. Chen, C. Jang, S. Xiao, M. Ishigami, and M. Fuhrer, *Nature Nanotech.* 2008, **3**, 206.
11. K. Kim, Y. Zhao, H. Jang, S. Lee, J. Kim, K. Kim, J. H. Ahn, P. Kim, J. Y. Choi and B. Hong, *Nature* 2009, **457**, 706.
12. A. A. Balandin, S. Ghosh, W. Bao, I. Calizo, D. Teweldebrhan, F. Miao, and C. N. Lau, *Nano Lett.* 2008, **8**, 902.
13. J. Hone, M. Whitney, C. Piskoti, and A. Zettl, *Phys. Rev. B* 1999, **59**, 2514.
14. H. Sevincli and G. Cuniberti, *Phys. Rev. B* 2010, **81**, 113401.
15. Z. W. Tan, J. S. Wang, and C. K. Gan, *Nano Lett.* 2011, **11**, 214.
16. Y. Ouyang and J. Guo, *Appl. Phys. Lett.* 2009, **94**, 263107.
17. H. Zhang, G. Lee, A. F. Fonseca, T. L. Borders, and K. Cho, *Journal of Nanomaterials*, 2010, **53**, 7657.
18. H. Kaneko, T. Ishiguro, A. Takahashi and J. Tsukamoto, *Synth. Met.* 1993, **57**, 4900.
19. E. R. Holland, S. J. Pomfret, P. N. Adams, L. Abell and P. Monkman, *Synth. Met.*, 1997, **84**, 777.
20. J. Li, X. Tang, H. Li, Y. Yan and Q. Zhang, *Synth. Met.*, 2010, **160**, 1153.
21. Y. Qi, Z. Wang, M. Zhang, F. Yang^a and X. Wang, *J. Mater. Chem. A*, 2013, **1**, 6110
22. J. R. Szczech, J. M. Higgins and S. Jin, *J. Mater. Chem.*, 2011, **21**, 4037.
23. R. Benoit, V. Hornebecq, F. Weill, L. Lecren, X. Bourrat and M. T. Delapierre, *J. Mater. Chem. A*, 2013, **1**, 14221
24. C. Yu, Y. S. Kim, D. Kim and J. C. Grunlan, *Nano Lett.*, 2008, **8**, 4428.
25. C. Bounioux, P. Diaz-Chao, M. Campoy-Quiles, M. S. Martin-Gonzalez, A. R. Goni, R. Yerushalmi-Rozen and C. Muller, *Energy Environ. Sci.*, 2013, **6**, 918.
26. Y. Lu, Y. Song, F. Wang, *Mater. Chem. Phys.*, 2013, **138**, 238.
27. Y. Du, S. Z. Shen, W. Yang, R. Donelson, K. Cai, P. S. Casey, *Synth. Met.*, 2012, **161**, 2688.
28. J. Xiang, L. and T. Drzal, *Polymer* 2012, **53**, 4202.
29. M. Scholdt, H. Do, J. Lang, A. Gall, A. Colmann, U. Lemmer, J. Koenig, M. Winkler and H. Boettner, *J. Electron. Mater.*, 2010, **39**, 1589.
30. H. Park, S. H. Lee, F. S. Kim, H. H. Choi, I. W. Cheong and J. H. Kim, *J. Mater. Chem. A*, 2014, **2**, 6532.
31. A. W. Musumeci, G. G. Silva, J. W. Liu and W. N. Martens, E. R. Waclawik, *Polymer*, 2007, **48**, 1667.
32. Y. Zhao, G. S. Tang, Z. Z. Yu and J. S. Qi, *Carbon*, 2012, **50**, 3064.
33. Y. W. Park, Y. S. Lee, C. Park, L. W. Shacklette and R. H. Baughman, *Solid State Commun.*, 1987, **63**, 1063.
34. K. Lee, S. Cho, H. P. Sung, A. J. Heeger, C. W. Lee and S. H. Lee, *Nature*, 2006, **441**, 65.
35. K. I. Winey and R. A. Vaia, *MRS Bull.*, 2007, **32**, 314.
36. R. D. Sherman, L. M. Middleman and S. M. Jacobs, *Polym. Eng. Sci.*, 1983, **23**, 36.
37. S. Kirkpatrick, *Rev. Mod. Phys.*, 1973, **45**, 574.
38. C. Fu, G. Zhao, H. Zhang, S. Li, *Int. J. Electrochem. Sci.* 2014, **9**, 46.
39. A. Dey, S. Panja, A. K. Sikder, S. Chattopadhyay, *RSC Adv.*, 2015, **5**, 10358.
40. S. Walia, S. Balendhran, H. Nili, S. Zhuiykov, G. Rosengarten, Q. H. Wang, M. Bhaskaran, S. Sriram, M. S. Strano, and K. Kalantar-zadeh, *Prog. Mat. Sci.* 2013, **58**(8), 1443-1489.
41. G. Zhou, D. W. Wang, F. Li, L. Zhang, N. Li, Z. S. Wu, L. Wen, G. Q. Lu and H. M. Cheng, *Chem. Mater.* 2010, **22**, 5306.
42. T. Mori, T. Nishimura, K. Yamaura, and E. T. Muromachi, *J. Appl. Phys.* 2007, **101**, 093714 (1-4),
43. C. Yu, K. Choi, L. Yin and J. C. Grunlan, *ACS Nano*, 2011, **5**, 7885.
44. M. He, F. Qiu, and Z. Lin, *Energy. Environ. Sci.* 2013, **6**, 1352
45. Y. S. Kim, D. Kim, K. J. Martin, C. Yu and J. C. Grunlan, *Macromol. Mater. Eng.* 2010, **295**, 431.
46. K. Choi, C. Yu, *PLOS one* 2012, **7**(9), e44977.
47. G. P. Moriarty, J. N. Wheeler, C. Yu and J. C. Grunlan, *Carbon* 2012, **50**, 885.

Journal Name

ARTICLE

48. A. Dey, J. Athar, P. Varma, H. Prasanth, A. K. Sikder, S. Chattopadhyay, *RSC Adv.*, 2015, **5**, 1950.
49. A. Dey, O.P.Bajpai, A.K.Sikder, S. Chattopadhyay, M.A.S. Khan, *Renewable, Sustainable Energy Reviews*, review article, **2015** (Accepted)